Repeated social defeat induces transient glial activation and brain hypometabolism: a PET imaging study

Author(s): Paula Kopschina Feltes, Erik FJ de Vries, Luis Eduardo Juarez-Orozco, Ewelina Kurtys, Rudi AJO Dierckx, Cristina Maria Moriguchi-Jeckel, Janine Doorduin.

CHAPTER 3

as published in the Journal of Cerebral Blood Flow & Metabolism. Kopschina Feltes et al. (2017) *Journal of Cerebral Blood Flow and Metabolism*. E-pub ahead of print. DOI: 10.1177/0271678X17747189.

Abstract

Psychosocial stress is a risk factor for the development of depression. Recent evidence suggests that glial activation could contribute to the development of depressive-like behaviour. This study aimed to evaluate *in vivo* whether repeated social defeat (RSD) induces short- and long-term inflammatory and metabolic alterations in the brain through positron emission tomography (PET). Male Wistar rats (n=40) were exposed to RSD by dominant Long-Evans rats on 5 consecutive days. Behavioural and biochemical alterations were assessed at baseline, day 5/6 and day 24/25 after the RSD protocol. Glial activation (^{11}C-PK11195 PET) and changes in brain metabolism (^{18}F-FDG PET) were evaluated on day 6, 11 and 25 (short-term), and at 3 and 6 months (long-term). Defeated rats showed transient depressive- and anxiety-like behaviour, increased corticosterone and brain IL-1β levels, as well as glial activation and brain hypometabolism in the first month after RSD. During the 3- and 6-month follow-up, no between-group differences in any investigated parameter were found. Therefore, non-invasive PET imaging demonstrated that RSD induces transient glial activation and reduces brain glucose metabolism in rats. These imaging findings were associated with stress-induced behavioural changes and support the hypothesis that neuroinflammation could be a contributing factor in the development of depression.

Keywords: brain metabolism, depression, neuroinflammation, PET imaging, repeated social defeat.

Introduction

Major depressive disorder (MDD) is a highly prevalent mental disorder affecting approximately 350 million people worldwide (1). Although MDD patients can benefit from treatment with antidepressants, over 30% of them are (at least partly) treatment-resistant (2). It is likely that the lack of treatment efficacy arises from the gaps in our understanding of MDD etiology (3).

One of the risk factors for the development of MDD is exposure to psychosocial stress. Currently, it is estimated that 20-25% of individuals exposed to highly stressful events develop MDD (4; 5). Notably, recent evidence suggests that (neuro)inflammatory processes may be involved in the physiopathology of MDD (6). In this sense, it is possible that psychosocial stress and persistent immunological activation might contribute (either additively or in parallel) to treatment resistance to conventional antidepressants (4; 7–11).

Microglia and astrocytes are involved in the immunological response of the central nervous system. These cells are known to undergo a series of events, commonly known as "glial activation", in response to brain disturbances such as neuronal damage or infection. These events include cell proliferation, morphological changes, increased expression of specific cell surface markers, production of cytokines and other inflammatory mediators (12). Depending on the type of stimulus and its duration, microglia activation can be classified as acute or chronic (13). Stress could be such a stimulus for glia activation. Glucocorticoids released as a consequence of psychosocial stress can bind to corticoid receptors on microglia and induce a shift towards a pro-inflammatory phenotype (14; 15). Chronically activated microglia produce well-known pro-inflammatory cytokines (16) such as interleukin-6 (IL-6), interleukin-1β (IL-1β) and tumour necrosis factor-α (TNF-α), all of which can affect the hypothalamic-pituitary-adrenal (HPA) axis and alter central serotonin levels (17) and thus could ultimately trigger mood disorders (18).

Nowadays, a widely accepted biomarker for activated microglia and astrocytes is the translocator protein (TSPO) (19). Under normal conditions, TSPO expression is low, but the receptor is highly overexpressed upon activation by an inflammatory stimulus. Therefore, TSPO overexpression has been used as a glial activation biomarker (20), measured noninvasively by means of positron emission tomography (PET) using ^{11}C-PK11195 as the tracer (21). At the same time, PET offers the possibility to image other (patho)physiological processes that are seemingly altered in MDD patients, such as brain glucose metabolism (22). Glucose metabolism can be measured with the tracer ^{18}F-FDG.

A growing body of preclinical evidence has implicated microglia activation in the neuroinflammatory response to psychosocial stress (23–26). Repeated social defeat (RSD) constitutes a model of psychosocial stress in rats with a high ethological validity (27). RSD is able to induce adverse physiological, behavioural and neuronal deficits, which resemble certain core symptoms of depression (9; 28). However, the effects of RSD on glial activation and brain metabolism have not been assessed *in vivo* and the long-term effects of RSD are largely unknown.

Therefore, the aim of this study was to longitudinally investigate the short- and long-term effects of psychosocial stress on the development of glial activation and brain metabolism in the RSD rat model of stress-induced depressive behaviour, using non-invasive PET imaging. To confirm the validity of the animal model, behavioural changes and corticosterone levels were assessed.

Materials and Methods

Experimental Animals

Male outbred Wistar Unilever rats (n=40, 8 weeks, 261±15g; Harlan, Horst, The Netherlands) were randomly divided in two groups: control (n=20) and social defeat (SoD, n=20). Sample size was calculated based on previous studies using ^{11}C-PK11195 PET for glial activation detection in rats (20; 29). The rats were individually housed during the experiment and kept in humidity-controlled, thermo-regulated (21±2°C) rooms under a 12:12 hour light:dark cycle with lights on at 7 a.m. After experimental day 25, rats were housed in pairs for the 6-month follow-up in order to prevent social isolation stress effects(30–32). Rats had *ad libitum* access to food and water, and were weighed every day.

Animal experiments were performed in accordance with the Dutch Experimental Animals Act (Wet op Dierenproeven; WoD) of 1977 and its later amendments. All procedures were approved by the Institutional Animal Care and Use Committee of the University of Groningen (Dier Experimenten Comissie – DEC), protocol DEC 6828A and 6828B, and are reported according to the ARRIVE guidelines (33).

Study design

The overall design of the study is depicted in detail on Fig. 1. Wistar rats (SoD group) were subjected to RSD on day 0–4. Controls were handled similarly, but not exposed to

aggressive residents. In each group, 10 rats were randomly selected for PET imaging and followed-up longitudinally with ^{11}C-PK11195 and ^{18}F-FDG on days -1, 6, 11 and 25 (same rats scanned with both tracers at all time points). Behavioural assessments were performed on days -2, 5 and 24 (short-term follow-up). The previously scanned rats were re-evaluated after 3 and 6 months (long-term follow-up) in order to determine the persistence of behavioural alterations, glial activation and differences in brain metabolism. During the follow up, the rats were weighed once a week.

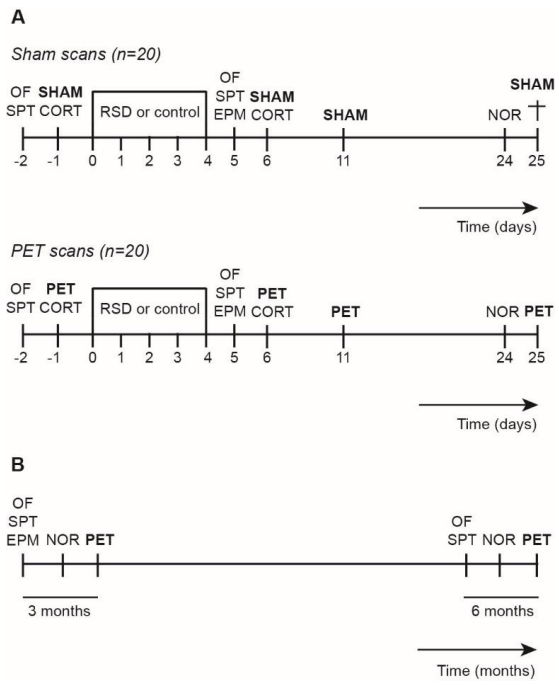

Figure 1: Study design. **(A)** Short-term follow-up: SoD (n=20) and control rats (n=20) were subjected to repeated social defeat from day 0–4. Open field (OF) and sucrose preference test (SPT) were carried out at day -2 and day 5. The elevated plus maze (EPM) was conducted on day 5. The novel object recognition test (NOR) was performed on day 24. PET scans with 11C-PK11195 and 18FFDG or sham scans were performed on day -1, 6, 11 and 25, with collection of serum samples for corticosterone (CORT) measurements on day -1 and 6. On day 25, 10 SoD and 10 control rats that underwent sham scans were terminated for brain collection and pro-inflammatory cytokines quantification. **(B)** Long-term follow-up: SoD (n=10) and control (n=10) rats were followed during six months after the cessation of RSD, with OF, SPT, EPM, NOR and PET scans being repeated after three and six months.

The remaining 10 rats per group were handled exactly the same, but were subjected to sham scans (anesthetized for the same period). On day 25, the rats that underwent sham scans were terminated and the brains were collected for the quantification of pro-inflammatory cytokines.

Repeated Social Defeat

SoD rats were introduced into the cage of a dominant (resident) male outbred Long Evans rat (502±36g; Harlan, Indianapolis, USA). The male Long Evans rats were housed in a separate experimental room in large cages (80x50x40 cm) with a Long Evans female rat, with ligated oviducts, to stimulate territorial aggression (27). The residents were trained and screened for aggressive behaviour at least three times prior to the experiment (8). Only residents that attacked an intruder within 1 min were used for the actual social defeat experiment.

The RSD experiment always took place between 16:00 and 18:00 p.m. Prior to RSD, females were removed from the cage of the resident. The experimental rat (intruder) was placed in the cage of the resident and they were allowed to interact for a period of 10 min or shorter if the intruder assumed a supine (submissive) position for at least 3 seconds. After submission (or 10 min exposure), the intruder was placed inside a wire mesh cage to avoid further physical contact, but still allowing intense visual, auditory and olfactory interactions for a total exposure period of 60 min. The social defeat protocol was repeated on 5 consecutive days using different residents. Control rats were placed in a new clean cage without resident for 60 min on 5 consecutive days.

Body weight gain (g)

Body weight gain (g) was calculated for each rat as the difference between the body weight at a given time point minus the weight on experimental day 0 (first day of RSD).

Behavioural Tests

Open field, elevated plus maze and novel object recognition tests were recorded on video for further analysis using Ethovision XT8.5 software (Noldus Information Technology, Wageningen, The Netherlands).

Sucrose Preference (SPT)

The sucrose preference test was used to assess anhedonia, a sign of depressive behaviour (8). Prior to the experiment, rats were habituated 4 times by exposure to a 1% sucrose solution for 1h. At baseline and after 5 days of RSD, a bottle with water and one with 1% sucrose solution were randomly placed in the cage of the rat. The preference for sucrose

was calculated as the total intake of sucrose solution divided by the total liquid intake and multiplied by 100% (34).

Open field (OF)

To investigate the effects of social defeat on explorative and anxiety-related behaviour, the rats were placed inside a square box (100x100x40 cm) for 10 min on day -2 and 5. The time spent in the centre of the arena relative to the time spent at the borders (a proxy measurement for anxiety), and the total distance moved (locomotor and explorative activity) were documented.

Elevated plus-maze (EPM)

A standard EPM with 52 cm arms extending from a 9x9 cm central area, 62 cm above the floor, was used to assess anxiety-like behaviour on day 5 and month 3 (35). Each session of 5 min was started by placing the rat in the central area facing the closed arms of the maze (36). The percentage of time spent in the open and closed arms, and in the centre was measured. The EPM could not be applied in the 6-month follow-up since the size of the animals impeded their mobility in the apparatus.

Novel object recognition (NOR)

A novel object recognition test was performed to evaluate visual memory (37) and the long-lasting memory impairment induced by RSD on day 24, month 3 and 6 (38). Rats were placed in a square box (50x50x40 cm) with two identical objects (plastic bottles or Lego cubes) (39). They were allowed to explore the objects for 3 min. The objects were removed and after 2 h one familiar and one new object were presented to the rat for 3 min. The preference index (PI) was calculated as the ratio between time spent on exploring the new object and the total time spent on object exploration (40).

Corticosterone Levels

For corticosterone quantification, rats were anesthetized with isoflurane mixed with medical air and 0.5 mL of whole blood was quickly collected from the tail vein on day -1 and 6. Samples were always collected at 10 a.m. The whole blood was allowed to cloth for 15 min and centrifuged at 6.000 rpm (3.5g) for 8 min at room temperature to obtain serum samples. Samples were stored at -20°C until further analysis by radioimmunoassay. Corticosterone (Sigma Chemical Co., Missouri, USA.) was used as

standard and ^{3}H-corticosterone as tracer (Perkin & Elmer, Massachusetts, USA). The sensitivity of the assay was 3 nM. The intra- and inter-assay variations were 6% and 9.6%, respectively.

PET Imaging

PET scans were performed using a small animal PET scanner (Focus 220, Siemens Medical Solutions, USA). Both ^{11}C-PK11195 and ^{18}F-FDG PET scans were performed on the same day for each investigated time point. ^{11}C-PK11195 PET scans were always carried out in the morning (between 10:00-11:00 a.m.). For the procedure, rats were anesthetized with isoflurane mixed with medical air (5% for induction, 2% for maintenance) and ^{11}C-PK11195 was injected via the penile vein (66±29 MBq, 1.4±2.3 nmol). Immediately after injection, rats were allowed to wake up and recover in their home cage. ^{18}F-FDG PET scans were carried out in the afternoon (between 15:00-16:00 p.m.), respecting an interval of at least 10 half-lives ($t^1/_2$) of ^{11}C isotope decay. Rats were deprived from food for 4-6 h, injected intraperitoneally (21; 41) with ^{18}F-FDG (31±8 MBq), and returned to their home cage afterwards. For both ^{11}C-PK11195 and ^{18}F-FDG PET, rats were anesthetized 45 min after tracer injection and placed in prone position into the camera with the head in the field of view. A 30-min static scan was acquired, the body temperature was maintained at 37°C with heating pads, heart rate and blood oxygen saturation were monitored, and eye salve was applied to prevent conjunctival dehydration. A transmission scan was obtained using a ^{57}Co point source for attenuation and scatter correction.

PET scans were iteratively reconstructed (OSEM2D, 4 iterations and 16 subsets) into a single frame after being normalized and corrected for attenuation and decay of radioactivity. Images with a 128x128x95 matrix, a pixel width of 0.632 mm, and a slice thickness of 0.762 mm were obtained. PET images were automatically co-registered to a functional ^{11}C-PK11195 or ^{18}F-FDG rat brain template (42), which was spatially aligned with a stereotaxic T2-weighted MRI template in Paxinos space (43) using VINCI 4.26 software (Max Planck Institute for Metabolism Research, Germany). Aligned images were resliced into cubic voxels (0.2 mm) and converted into standardized uptake value (SUV) images: SUV= [tissue activity concentration (MBq/g) x body weight (g)] / [injected dose (MBq)], assuming a tissue density of 1 g/ml. ^{18}F-FDG uptake was not corrected for blood glucose levels (21; 44).

Tracer uptake was calculated in several predefined volumes-of-interest (VOI). VOIs were selected based on previous findings (22; 23; 45–51), taking the size of the brain regions into consideration. Due to the limited resolution of the small animal PET scanner (1.4 mm) (52), small brain regions were excluded to minimize partial volume effects (53). Therefore, the investigated regions were the amygdala/piriform complex, brainstem, cerebellum, cingulate cortex, entorhinal cortex, frontal association cortex, hippocampus, hypothalamus, insular cortex, medial prefrontal cortex, motor/somatosensory cortex, orbitofrontal cortex and striatum.

Enzyme linked immunoassay (ELISA) for pro-inflammatory cytokines in the brain

On day 25, rats were terminated under deep anaesthesia by transcardial perfusion with phosphate-buffered saline pH 7.4. Brains were collected and rapidly frozen and stored at -80°C. Frontal cortex, hippocampus, cerebellum and parietal/temporal/occipital cortex were dissected and prepared as published (39). Pro-inflammatory cytokines IL-6, TNF-α (Biolegend, San Diego, USA) and IL-1β (Thermo Scientific, Rockford, USA) concentrations were determined by ELISA according to the manufacturer's instructions. Total protein concentration in the brain areas was quantified through Bradford Assay and the cytokine levels corrected for the amount of protein after measurement (54).

Statistical Analysis

Statistical analyses were performed with the SPSS software (IBM Corp. Released 2013. IBM SPSS Statistics for Windows, Version 22.0. Armonk, NY). Continuous data are expressed as mean ± standard error of the mean (SEM). Data expressed as percentage were square root arcsine transformed prior to statistical analysis (55; 56). Differences in variables from behavioural and biochemical tests were tested through a two-sided paired or independent samples *t-test* and the effect size of the differences between groups was calculated through Cohen's *d* (57; 58). The Generalized Estimating Equations (GEE) model (59) was used to account for repeated measurements in the longitudinal design and missing data in body weight and PET measurements. For the statistical model of the body weight gain, "group", "day of measurement" and the interaction "group × day of measurement" were included as variables. The GEE model for ^{11}C-PK11195 and ^{18}F-FDG uptake (SUV) was applied individually for each brain region, including the variables "group", "day of scan" and the interaction "group × day of scan" in the model. The data was further explored through pairwise comparison of "group × day of scan" in each brain

region for all scan time points combined. The AR(1) working correlation matrix was selected according to the quasi-likelihood under the independence model information criterion value. Wald's statistics and associated *p*-values were considered statistically significant at $p<0.05$. A Bonferroni-Holm correction was used to adjust significance levels for multiple comparisons (60).

Results

As a consequence of methodological issues, 2 control rats did not survive a PET scan and a humane endpoint was applied to one rat due to a lethal wound during the RSD protocol.

RSD reduced bodyweight gain, normalizing only after 5 weeks

The bodyweight of the rats was measured daily until day 25 and weekly thereafter. No significant differences in bodyweight between groups was found before the start of RSD (control: 266±19g, and SoD: 261±18g, $p=0.44$). For the first 25 days, a significant main effect was found for the factors group ($p<0.001$) and day of measurement ($p<0.001$), and for the interaction group × day of measurement ($p<0.001$), showing that RSD significantly reduced bodyweight gain. More specifically, the reduction in bodyweight gain was already apparent on experimental day 2 (control: 8.8±1.4g vs. SoD: 4.2±1.3g, $p=0.01$), with no recovery to control levels until day 25 (control: 100.9±3.9g vs. SoD: 80.8±2.8g, $p<0.001$). When comparing the bodyweight gain from 5 weeks after the RSD until week 28 (6 months), there was a statistically significant main effect on day of measurement ($p<0.001$), and in the interaction day of measurement × group ($p<0.001$), but no difference was found between groups (Supplementary Fig. 1).

RSD provoked acute anxiety-like and depressive-like behaviour without cognition impairment

Behavioural tests were performed at baseline and at several time-points after RSD. Social defeat caused a reduced preference for sucrose (Fig. 2-A). At baseline, rats had a 96±1% preference for sucrose, whereas after the RSD (day 5) the preference decreased to 74±4% ($p<0.001$, $d=1.1$). At the 3- and 6-month follow up the sucrose preference of the SoD group was restored to the baseline value (Fig. 2-B). The sucrose preference of the control group remained constant over time.

The anxiety-like behaviour and explorative activity were investigated at baseline and immediately after the RSD protocol (day 5), using the OF. No significant differences

between groups were found at baseline for distance moved (control: 3.8±0.2m vs. SoD: 3.8±0.2m, p=0.83, d=0.01) and time spent in the centre of the arena (control: 89±7s vs. SoD: 80±7s, p=0.49, d=0.2). On day 5, rats exposed to RSD demonstrated anxiety-like behaviour through decreased exploration (control: 3.4±0.3m vs. SoD: 2.6±0.2m, p<0.001, d=0.7) and a diminished time spent in the centre of the arena (control: 63±13s vs. SoD: 42±10s, p<0.001, d=0.5) when compared to controls (Fig. 2-C and 2-D). At 3 and 6 months after RSD, the anxiety-like behaviour of SoD rats had normalized, as the OF test did not reveal any significant difference between groups (Fig. 2-E and 2-F).

Anxiety-like behaviour was additionally assessed with the EPM. On day 5, rats in the SoD group spent a significantly lower percentage of time in the open arms (control: 14±2% vs. SD: 9±2%, p<0.05, d=0.6) and a higher percentage of time in the closed arms (control: 61±3% vs. SD: 71±4%, p<0.05, d=0.7) as compared to controls, showing that rats exposed to RSD were more anxious. No significant difference between groups in time spent in the centre was found (control: 25±2% vs. SoD: 20±2%, p=0.114, d=0.6; Fig. 1-G). No significant difference between groups was observed anymore at month 3 (Fig. 2-H).

To assess whether RSD had long-lasting effects on memory, the NOR test was performed on day 24, month 3 and 6. No significant differences were found between groups (Fig. 2-I and 2-J).

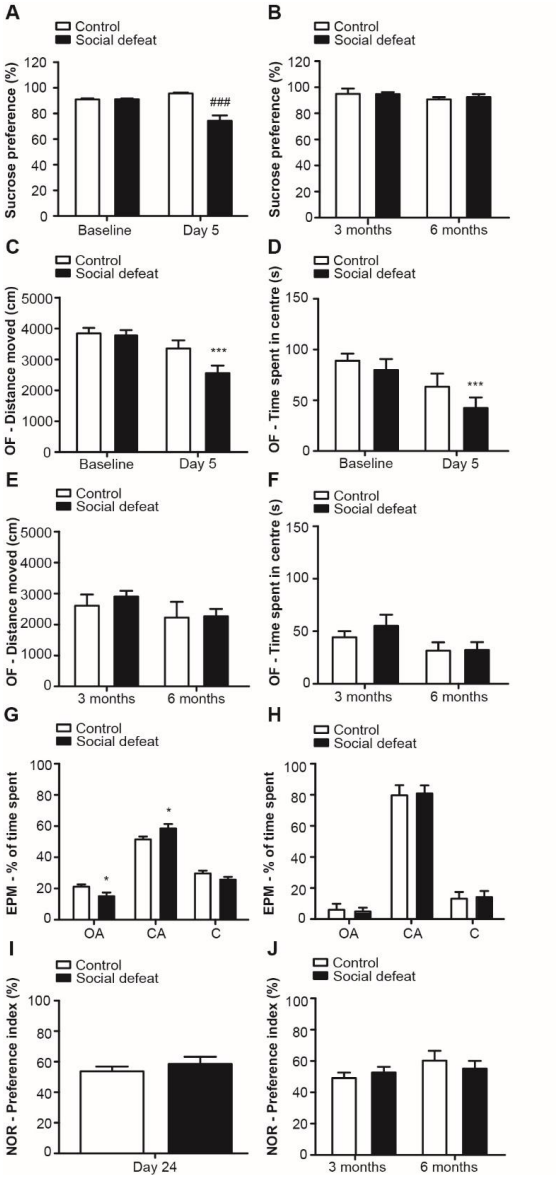

Figure 2: RSD-induced behavioural alterations in SoD rats in the short-term follow-up. **(A)** Anhedonic-like behaviour was demonstrated in SoD rats through a within-group comparison of the sucrose preference test (SPT) on baseline and day 5, $^{###}p<0.001$. **(B)** No differences in SPT of control and SoD rats on the 3- and 6-month follow-up. Anxiety-like behaviour was demonstrated in SoD rats in the open field test (OF) through **(C)** decreased distance moved on day 5 as compared to control rats, $***p<0.001$ and **(D)** decreased total time spent in the centre of the arena, $***p<0.001$. In the 3- and 6-month follow-up, **(E)** no differences were found in distance moved or **(F)** time spent in the centre of the OF arena between groups. The elevated plus maze (EPM) confirmed the anxiety behaviour of SoD rats on day 5, with **(G)** decreased the percentage of time spent in the open arms (OA), $*p<0.05$, and increased the percentage of time spent in the closed arms (CA), $*p<0.05$. No differences were found regarding the percentage of time spent in the centre (C). **(H)** In the 3-month evaluation, no differences were found in the percentage of time spent in the OA, CA or C between groups. RSD did not affect cognition, measured through the novel object recognition (NOR) test

and expressed as percentage of preference index (PI). **(I)** No between group difference on PI was found on day 24. **(J)** PI was not significantly different between groups on the 3- and 6-month follow-up.

Serum corticosterone increased significantly in response to social defeat

Serum concentrations of corticosterone were measured before (day -1) and after RSD (day 6). No significant differences were found between groups on day -1 (ctrl: 235±45 nmol/L vs. SoD: 186±43 nmol/L, p=0.44). Socially defeated rats had significantly increased corticosterone levels after the RSD (day -1: 186±43 nmol/L vs. day 6: 560±114 nmol/L, $p<0.01$, $d=1.00$), whereas corticosterone levels in control rats were not affected (day -1: 235±45 nmol/L vs. day 6: 207±40 nmol/L, $p=0.675$, $d=0.1$).

Stress-induced glial activation was detected at short-term follow-up after RSD but not at long-term

Between-group comparison of the ^{11}C-PK11195 PET data revealed no significant differences in tracer uptake between groups at baseline or immediately after RDS (day 6). However, an increased tracer uptake (suggestive of the presence of activated glial cells) was observed in defeated rats on experimental day 11 and 25 (Table 1). The regions that presented significantly increased uptake on day 11 were the orbitofrontal cortex (+38%, $p<0.001$), entorhinal cortex (+30%, $p=0.001$), insular cortex (+30%, $p=0.002$), medial prefrontal cortex (+26%, $p<0.001$) and cerebellum (+23%, $p=0.001$), as compared to the control group (Fig 3-A). On day 25, only the frontal association cortex had increased uptake (+23%, $p=0.008$). Furthermore, no between-group differences in ^{11}C-PK11195 uptake were found in any brain region at months 3 and 6. Analysis of the effect of time on tracer uptake in brain regions of control and defeated rats revealed a global increase in the uptake of ^{11}C-PK11195 at month 3 and 6 when compared to baseline levels (Table 2).

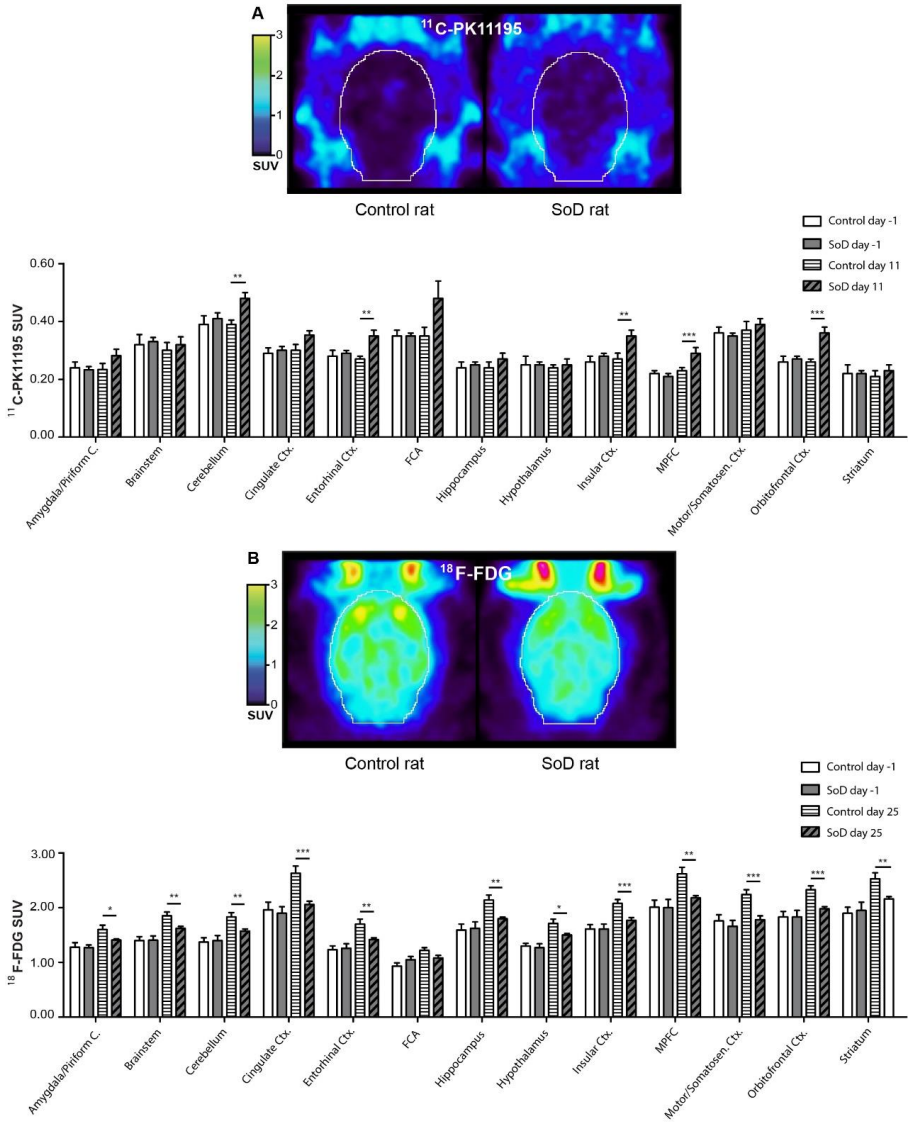

Figure 3: (A) ^{11}C-PK11195 PET scan of a representative control and defeated rat on experimental day 11, followed by a graphical representation of ^{11}C-PK11195 SUV on baseline and day 11. *p<0.05, **p<0.01 and ***p<0.001. **(B)** ^{18}F-FDG PET scan of a representative control and defeated rat on experimental day 25, followed by a graphical representation of ^{18}F-FDG SUV on baseline and day 25. *p<0.05, **p<0.01 and ***p<0.001.

Brain glucose metabolism alterations in defeated rats found at short-term follow-up normalized within 3 months

Several brain regions demonstrated alterations in brain glucose metabolism in SoD rats (Table 3). On day 6, SoD rats had lower ^{18}F-FDG uptake in the motor/somatosensory (-19%, p=0.006), cingulate (-17%, p=0.03) and entorhinal cortex (-17%, p=0.04) than controls. On day 25 (Fig. 3-B), a global decrease in tracer uptake was found in the cingulate cortex (-22%, p<0.001), motor/somatosensory cortex (-21%, p<0.001), medial prefrontal cortex (-17%, p=0.001), entorhinal cortex (-16%, p=0.006), hippocampus (-16%, p=0.001), insular cortex (-15%, p<0.001), orbitofrontal cortex (-15%, p<0.001), striatum (-15%, p=0.002), cerebellum (-14%, p=0.009), hypothalamus (-13%, p=0.013), brainstem (-12%, p=0.003) and amygdala/piriform complex (-11%, p=0.024). In contrast, no differences in ^{18}F-FDG uptake between groups were observed at baseline, 3 months or 6 months after RDS.

Table 1 – ^{11}C-PK11195 SUV values of the short-term follow-up for individual brain regions of control (n=8) and SoD (n=9) rats at baseline, day 6, 11 and 25.

	Baseline			Day 6			Day 11			Day 25		
	Control	SoD		Control	SoD		Control	SoD		Control	SoD	
Brain Regions	**Mean ± SE**	**Mean ± SE**	***p***	**Mean ± SE**	**Mean ± SE**	***p***	**Mean ± SE**	**Mean ± SE**	***p***	**Mean ± SE**	**Mean ± SE**	***p***
Amygdala/Piriform complex	0.24 ± 0.02	0.23 ± 0.02	n.s	0.23 ± 0.02	0.23 ± 0.01	n.s	0.23 ± 0.01	0.28 ± 0.02	n.s	0.25 ± 0.02	0.24 ± 0.02	n.s
Brainstem	0.32 ± 0.04	0.33 ± 0.01	n.s	0.31 ± 0.03	0.32 ± 0.02	n.s	0.30 ± 0.02	0.32 ± 0.03	n.s	0.32 ± 0.04	0.31 ± 0.03	n.s
Cerebellum	0.39 ± 0.03	0.41 ± 0.02	n.s	0.41 ± 0.03	0.47 ± 0.03	n.s	0.39 ± 0.02	0.48 ± 0.02	0.001	0.45 ± 0.03	0.51 ± 0.04	n.s
Cingulate cortex	0.29 ± 0.02	0.30 ± 0.01	n.s	0.30 ± 0.01	0.33 ± 0.02	n.s	0.30 ± 0.02	0.35 ± 0.02	n.s	0.34 ± 0.02	0.41 ± 0.02	n.s
Entorhinal cortex	0.28 ± 0.02	0.29 ± 0.01	n.s	0.29 ± 0.03	0.30 ± 0.02	n.s	0.27 ± 0.01	0.35 ± 0.02	0.001	0.31 ± 0.03	0.31 ± 0.02	n.s
Frontal association cortex	0.35 ± 0.02	0.35 ± 0.01	n.s	0.33 ± 0.02	0.35 ± 0.01	n.s	0.35 ± 0.03	0.48 ± 0.06	n.s	0.34 ± 0.02	0.42 ± 0.02	0.008
Hippocampus	0.24 ± 0.02	0.25 ± 0.01	n.s	0.25 ± 0.02	0.28 ± 0.02	n.s	0.24 ± 0.02	0.27 ± 0.02	n.s	0.28 ± 0.03	0.29 ± 0.02	n.s
Hypothalamus	0.25 ± 0.03	0.25 ± 0.01	n.s	0.26 ± 0.02	0.26 ± 0.01	n.s	0.24 ± 0.01	0.25 ± 0.02	n.s	0.29 ± 0.04	0.29 ± 0.02	n.s
Insular cortex	0.26 ± 0.02	0.28 ± 0.01	n.s	0.26 ± 0.02	0.28 ± 0.01	n.s	0.27 ± 0.02	0.35 ± 0.02	0.002	0.27 ± 0.03	0.27 ± 0.02	n.s
Medial Prefrontal cortex	0.22 ± 0.01	0.21 ± 0.01	n.s	0.23 ± 0.02	0.26 ± 0.01	n.s	0.23 ± 0.01	0.29 ± 0.02	<0.001	0.25 ± 0.03	0.32 ± 0.02	n.s
Motor/Somatosensory cortex	0.36 ± 0.02	0.35 ± 0.01	n.s	0.36 ± 0.02	0.37 ± 0.02	n.s	0.37 ± 0.03	0.39 ± 0.02	n.s	0.43 ± 0.02	0.48 ± 0.03	n.s
Orbitofrontal cortex	0.26 ± 0.02	0.27 ± 0.01	n.s	0.26 ± 0.01	0.29 ± 0.02	n.s	0.26 ± 0.01	0.36 ± 0.02	<0.001	0.27 ± 0.02	0.31 ± 0.02	n.s
Striatum	0.22 ± 0.03	0.22 ± 0.01	n.s	0.23 ± 0.02	0.23 ± 0.02	n.s	0.21 ± 0.02	0.23 ± 0.02	n.s	0.26 ± 0.03	0.25 ± 0.02	n.s

Table 2 – Effect of time in ^{11}C-PK11195 uptake values in control (n=8) and SoD (n=9) rats during the long-term follow-up (3 and 6 months) for individual brain regions as compared to baseline uptake levels.

	Control					SoD				
	Day -1	3 months		6 months		Day -1	3 months		6 months	
Brain Regions	**Mean ± SE**	**Mean ± SE**	***P***	**Mean ± SE**	***p***	**Mean ± SE**	**Mean ± SE**	***p***	**Mean ± SE**	***p***
Amygdala/Piriform complex	0.24 ± 0.02	0.31 ± 0.01	0.005	0.35 ± 0.01	<0.001	0.23 ± 0.02	0.29 ± 0.01	0.001	0.33 ± 0.01	<0.001
Brainstem	0.32 ± 0.04	0.42 ± 0.03	0.011	0.49 ± 0.03	<0.001	0.33 ± 0.01	0.40 ± 0.01	0.001	0.47 ± 0.01	<0.001
Cerebellum	0.39 ± 0.03	0.55 ± 0.03	<0.001	0.61 ± 0.02	<0.001	0.41 ± 0.02	0.61 ± 0.02	<0.001	0.65 ± 0.04	<0.001
Cingulate cortex	0.29 ± 0.02	0.48 ± 0.02	<0.001	0.55 ± 0.04	<0.001	0.30 ± 0.01	0.48 ± 0.02	<0.001	0.56 ± 0.03	<0.001
Entorhinal cortex	0.28 ± 0.02	0.33 ± 0.02	0.008	0.37 ± 0.01	<0.001	0.29 ± 0.01	0.34 ± 0.01	0.001	0.35 ± 0.01	<0.001
Frontal association cortex	0.35 ± 0.02	0.43 ± 0.04	n.s.	0.45 ± 0.04	0.012	0.35 ± 0.01	0.45 ± 0.02	<0.001	0.49 ± 0.03	<0.001
Hippocampus	0.24 ± 0.02	0.36 ± 0.02	<0.001	0.42 ± 0.01	<0.001	0.25 ± 0.01	0.38 ± 0.01	<0.001	0.42 ± 0.01	<0.001
Hypothalamus	0.25 ± 0.03	0.37 ± 0.02	0.001	0.44 ± 0.02	<0.001	0.25 ± 0.01	0.32 ± 0.02	0.020	0.39 ± 0.01	<0.001
Insular cortex	0.26 ± 0.02	0.32 ± 0.02	0.006	0.37 ± 0.02	<0.001	0.28 ± 0.01	0.32 ± 0.01	n.s.	0.34 ± 0.01	<0.001
Medial Prefrontal cortex	0.22 ± 0.01	0.40 ± 0.03	<0.001	0.46 ± 0.03	<0.001	0.21 ± 0.01	0.40 ± 0.01	<0.001	0.48 ± 0.02	<0.001
Motor/Somatosensory cortex	0.36 ± 0.02	0.53 ± 0.03	<0.001	0.56 ± 0.04	<0.001	0.35 ± 0.01	0.53 ± 0.03	<0.001	0.56 ± 0.03	<0.001
Orbitofrontal cortex	0.26 ± 0.02	0.36 ± 0.02	<0.001	0.41 ± 0.02	<0.001	0.27 ± 0.01	0.39 ± 0.01	<0.001	0.44 ± 0.02	<0.001
Striatum	0.22 ± 0.03	0.34 ± 0.01	<0.001	0.40 ± 0.01	<0.001	0.22 ± 0.01	0.34 ± 0.01	<0.001	0.40 ± 0.01	<0.001

A within-group comparison in control rats showed a significant increase in the ^{18}F-FDG uptake in all investigated brain regions on day 6 and 25, as compared to baseline levels (Table 4). In SoD rats, increased ^{18}F-FDG uptake was only found on day 25 in the brainstem (+13%, p=0.009), entorhinal cortex (+13%, p=0.03) and hypothalamus (+10%, p=0.016). Further analysis of the effect of time in the long-term follow-up showed a significant increase in ^{18}F-FDG in all brain regions for both groups at month 3 and 6, as compared to baseline.

Elevated IL-1β levels were found in the frontal cortex 3 weeks after RSD

A significant increase in the levels of IL-1β was found in the frontal cortex of defeated rats (Supplementary Fig. 2-A), when compared to control rats (controls: 74±6 pg/mg vs. SoD: 122±14 pg/mg, p=0.012, d=1.55) at day 25. No differences between groups were found in hippocampus, cerebellum and parietal/temporal/occipital cortex. No significant differences in IL-6 and TNF-α levels (p≥0.05) were found in any of the brain regions (Supplementary Fig. 2-B and C). However, the Cohen's effect size values for IL-6 and TNF-α levels in frontal cortex (d=0.63 and 0.55, respectively) suggest a trend towards increased expression of these cytokines.

Table 3 - ^{18}F-FDG SUV values of the short-term follow-up for individual brain regions of control (n=8) and SoD (n=9) rats at baseline, day 6, 11 and 25.

	Baseline			Day 6			Day 11			Day 25		
	Control	SoD		Control	SoD		Control	SoD		Control	SoD	
Brain Regions	**Mean ± SE**	**Mean ± SE**	***p***	**Mean ± SE**	**Mean ± SE**	***P***	**Mean ± SE**	**Mean ± SE**	***p***	**Mean ± SE**	**Mean ± SE**	***p***
Amygdala/Piriform complex	1.28 ± 0.08	1.27 ± 0.05	n.s.	1.45 ± 0.07	1.28 ± 0.07	n.s.	1.28 ± 0.06	1.43 ± 0.12	n.s.	1.60 ± 0.08	1.41 ± 0.02	0.024
Brainstem	1.40 ± 0.07	1.41 ± 0.08	n.s.	1.64 ± 0.09	1.47 ± 0.07	n.s.	1.47 ± 0.08	1.68 ± 0.12	n.s.	1.85 ± 0.07	1.62 ± 0.04	0.003
Cerebellum	1.37 ± 0.08	1.40 ± 0.09	n.s.	1.65 ± 0.08	1.48 ± 0.09	n.s.	1.47 ± 0.09	1.67 ± 0.13	n.s.	1.83 ± 0.08	1.57 ± 0.04	0.009
Cingulate cortex	1.96 ± 0.14	1.90 ± 0.12	n.s.	2.30 ± 0.13	1.90 ± 0.12	0.030	1.97 ± 0.15	2.11 ± 0.16	n.s.	2.63 ± 0.13	2.06 ± 0.06	<0.001
Entorhinal cortex	1.23 ± 0.07	1.26 ± 0.08	n.s.	1.49 ± 0.09	1.24 ± 0.07	0.040	1.27 ± 0.07	1.42 ± 0.11	n.s.	1.70 ± 0.09	1.42 ± 0.03	0.006
Frontal association cortex	0.98 ± 0.06	1.05 ± 0.06	n.s.	1.16 ± 0.07	1.11 ± 0.06	n.s.	0.98 ± 0.06	1.18 ± 0.07	n.s.	1.22 ± 0.05	1.08 ± 0.05	n.s.
Hippocampus	1.59 ± 0.11	1.62 ± 0.12	n.s.	1.90 ± 0.11	1.67 ± 0.11	n.s.	1.66 ± 0.10	1.85 ± 0.15	0.030	2.14 ± 0.09	1.80 ± 0.03	0.001
Hypothalamus	1.30 ± 0.05	1.27 ± 0.07	n.s.	1.49 ± 0.09	1.32 ± 0.08	n.s.	1.32 ± 0.08	1.50 ± 0.11	n.s.	1.71 ± 0.08	1.50 ± 0.03	0.013
Insular cortex	1.61 ± 0.08	1.61 ± 0.09	n.s.	1.90 ± 0.10	1.66 ± 0.09	n.s.	1.66 ± 0.09	1.79 ± 0.15	0.030	2.08 ± 0.07	1.77 ± 0.05	<0.001
Medial Prefrontal cortex	2.01 ± 0.13	2.00 ± 0.15	n.s.	2.31 ± 0.13	2.03 ± 0.14	n.s.	2.03 ± 0.14	2.26 ± 0.17	n.s.	2.62 ± 0.12	2.18 ± 0.04	0.001
Motor/Somatosensory cortex	1.76 ± 0.11	1.66 ± 0.11	n.s.	2.06 ± 0.11	1.67 ± 0.09	0.006	1.79 ± 0.10	1.86 ± 0.13	n.s.	2.24 ± 0.09	1.78 ± 0.07	<0.001
Orbitofrontal cortex	1.83 ± 0.10	1.83 ± 0.12	n.s.	2.09 ± 0.11	1.89 ± 0.12	n.s.	1.81 ± 0.11	2.06 ± 0.15	0.003	2.33 ± 0.07	1.98 ± 0.04	<0.001
Striatum	1.90 ± 0.11	1.95 ± 0.15	n.s.	2.22 ± 0.12	1.94 ± 0.13	n.s.	1.94 ± 0.12	2.18 ± 0.18	n.s.	2.53 ± 0.11	2.16 ± 0.04	0.002

Table 4 - Effect of time in ^{18}F-FDG SUV values in control (n=8) and SoD (n=9) rats during the long-term follow-up (3 and 6 months).

	Control					SoD				
	Day -1	3 months		6 months		Day -1	3 months		6 months	
Brain Regions	**Mean ± SE**	**Mean ± SE**	***p***	**Mean ± SE**	***p***	**Mean ± SE**	**Mean ± SE**	***P***	**Mean ± SE**	***p***
Amygdala/Piriform complex	1.27 ± 0.05	1.59 ± 0.04	<0.001	1.81 ± 0.08	<0.001	1.28 ± 0.08	1.78 ± 0.10	0.001	1.91 ± 0.10	<0.001
Brainstem	1.40 ± 0.07	1.87 ± 0.04	<0.001	2.15 ± 0.09	<0.001	1.41 ± 0.08	2.06 ± 0.10	<0.001	2.17 ± 0.11	<0.001
Cerebellum	1.37 ± 0.08	1.93 ± 0.05	<0.001	2.21 ± 0.10	<0.001	1.40 ± 0.08	2.16 ± 0.12	<0.001	2.27 ± 0.14	<0.001
Cingulate cortex	1.96 ± 0.14	2.63 ± 1.10	0.001	2.92 ± 0.17	<0.001	1.90 ± 0.14	2.82 ± 0.17	<0.001	2.99 ± 0.16	<0.001
Entorhinal cortex	1.23 ± 0.07	1.76 ± 0.05	<0.001	2.01 ± 0.11	<0.001	1.26 ± 0.07	1.95 ± 0.12	<0.001	2.12 ± 0.12	<0.001
Frontal association cortex	0.98 ± 0.06	1.19 ± 0.04	0.004	1.39 ± 0.04	<0.001	1.05 ± 0.06	1.28 ± 0.05	0.005	1.40 ± 0.06	<0.001
Hippocampus	1.59 ± 0.11	2.14 ± 0.07	<0.001	2.42 ± 0.12	<0.001	1.62 ± 0.12	2.38 ± 0.13	<0.001	2.54 ± 0.15	<0.001
Hypothalamus	1.30 ± 0.05	1.75 ± 0.06	<0.001	2.01 ± 0.09	<0.001	1.27 ± 0.07	2.00 ± 0.11	<0.001	2.13 ± 0.11	<0.001
Insular cortex	1.61 ± 0.08	2.03 ± 0.04	<0.001	2.30 ± 0.09	<0.001	1.61 ± 0.09	2.08 ± 0.10	0.003	2.21 ± 0.10	<0.001
Medial Prefrontal cortex	2.01 ± 0.13	2.61 ± 0.10	0.001	2.97 ± 0.14	<0.001	2.00 ± 0.15	2.89 ± 0.16	<0.001	3.07 ± 0.17	<0.001
Motor/Somatosensory cortex	1.76 ± 0.11	2.24 ± 0.06	0.001	2.50 ± 0.11	<0.001	1.66 ± 0.11	2.26 ± 0.11	<0.001	2.37 ± 0.10	<0.001
Orbitofrontal cortex	1.83 ± 0.10	2.20 ± 0.06	0.005	2.50 ± 0.08	<0.001	1.83 ± 0.12	2.39 ± 0.11	0.004	2.54 ± 0.13	<0.001
Striatum	1.90 ± 0.11	2.55 ± 0.07	<0.001	2.82 ± 0.15	<0.001	1.95 ± 0.15	2.86 ± 0.16	<0.001	3.00 ± 0.17	<0.001

Discussion

For the first time, we have demonstrated *in vivo* that psychosocial stress in rats transiently induces depressive- and anxiety-like behaviour associated with glial activation and altered brain glucose metabolism, as measured by PET. Yet, these effects had normalized during the 3 and 6 months follow-up.

The RSD protocol effectively exposed rats to recurrent stress as was confirmed by increased corticosterone levels, decreased bodyweight gain, and depressive- and anxiety-like behaviour. These findings are in line with previous studies, confirming the validity of the model (8; 61–63). However, we now observed for the first time that these effects of RSD on bodyweight and behaviour did not persist at 3 and 6 months after RSD. Furthermore, we observed that defeated rats did not reveal long-lasting memory deficits measurable in the NOR test. Previous studies focused on the cognitive alterations shortly after the termination of the stressful condition and reported that high levels of corticosterone impaired object recognition memory (64–66). Although we found that corticosterone levels were elevated 2 days after the 5-day RSD protocol, we did not measure corticosterone levels at the time of the NOR test (day 24). It is plausible that corticosterone levels had already normalized 3 weeks after RSD. A recent study by McKim et al. (67) subjected mice to RSD for six consecutive days and tested the effects on memory with the Barnes maze. They reported an increased number of errors to find the escape hole of the maze for defeated rats at day 2, but not at day 28. Put together, these results suggest that RSD causes only early, transient deficits in short-term memory recall (67).

PET imaging with the TSPO tracer ^{11}C-PK11195 demonstrated the presence of glial activation 7 days after RSD in the cerebellum, entorhinal cortex, insular cortex, medial prefrontal cortex and the orbitofrontal cortex. The medial prefrontal cortex and orbitofrontal cortex are associated with depressive behaviour and reward (68; 69), whereas the cerebellum and insular cortex have been related to anxiety (48; 70; 71), and the entorhinal cortex is linked with conscious memory and spatial navigation (71; 72). Three weeks after RSD, glial activation was only evident in the frontal association cortex, a brain area associated with depression (73). Interestingly, increased levels of IL-1β were temporally and spatially consistent with this glial activation. IL-1β seems to be the key mediator between increased corticosterone levels as a consequence of psychosocial stress and neuroinflammatory processes (15; 74–76). Overall, the observed glial activation was in accordance with previous preclinical studies that have evaluated brain cytokine

expression in conjunction with microglia activation after RSD (9; 77; 78). However, in the 3- and 6-month follow-up of our study, no differences in tracer uptake between groups were detected anymore, indicating that RSD-induced glial activation is transient.

We observed that ^{18}F-FDG brain uptake was decreased in the motor cortex of SoD rats on day 6, which is in agreement with the decreased locomotor activity observed in the OF test. The decreased ^{18}F-FDG uptake in the cingulate cortex combined with the reduced sucrose preference suggests that RSD reduced motivation and induced anhedonia (79). Overall, the global decrease in ^{18}F-FDG uptake in the brain of SoD rats on day 25 is in line with the results reported in unipolar depressive patients (22; 80–82).

An interesting insight arises from the finding that longitudinal within-group comparisons revealed an increase in ^{11}C-PK11195 uptake over a 6-month time period both in control and SoD rats. This is in agreement with previous studies that demonstrated age-related microglia activation in healthy rodents (83) and humans (84). There was also a time-related increase in ^{18}F-FDG uptake, which differed between groups. In contrast to controls, SoD rats had a stable uptake during the short-term follow-up, which only reached the levels of the control group during the long-term follow-up. This suggests that RSD delays rather than hampers brain metabolism maturation (85).

Our most interesting finding was the seemingly “transient” nature of the effects of RSD. However, this does not mean that there are no long-term effects of RDS at all, and further efforts should be encouraged into elucidating whether the observed transient changes are leading to other deleterious effects. To our knowledge, this is the first study that reports a 6-month follow-up after RSD along with non-invasive (PET) imaging evaluation. Buwalda et al. evaluated the long-term effects (3 months) of adolescent exposure to RSD (86) and showed no differences between controls and defeated animals in physiological (body temperature and corticosterone levels) and behavioural (EPM and social interaction) parameters. These findings are in agreement with our study that also did not reveal any long-lasting negative behavioural effects of social defeat (or at least, not measurable with the reported methods). Still, the question remains whether exposure to psychosocial stress conveys hitherto uninvestigated long-term effects mediated by (neuro)inflammation, which may be relevant in the pathogenesis and treatment of (treatment-resistant) MDD.

Due to its longitudinal design, this study has some limitations. First, we did not confirm PET findings by immunohistochemical analysis of alterations in the morphology of microglia and/or astrocytes. However, indirect measurement of the pro-inflammatory

glial phenotype was confirmed by the quantification of pro-inflammatory cytokines in the brain on day 25. Second, corticosterone levels were only measured in serum during two timepoints (before and immediately after RSD) in order to confirm the biochemical effect of the RSD protocol in the model. Therefore, we do not have any information about the longitudinal changes in corticosterone levels during the whole period of the study. Third, recent studies have shown that the TSPO tracer ^{11}C-PK11195 is not the most sensitive candidate for detecting mild glial activation. Tracers like ^{11}C-CB184 (87), ^{11}C-PBR28 (20) and ^{18}F-DPA-714 (88) are second generation TSPO tracers with superior characteristics in comparison with ^{11}C-PK11195 in terms of affinity and/or nonspecific binding. Therefore, for future preclinical studies, a second generation TSPO tracer should be considered. The second generation, however, are sensitive to polymorphism in the TSPO receptor in humans. Forth, the SUV is a semi-quantitative measurement of tracer uptake, with the advantage of enabling individual monitoring over time and simplicity of the analysis (89). However, the SUV is sensitive for changes such as blood flow and tracer delivery. Moreover, it is positively correlated to the subject's body weight. To overcome differences in body weight that might influence SUV values, it has been clinically proposed to use the body surface area or lean body mass instead of body weight in the SUV equation (90). However, this was not validated in the preclinical setting. Additionally, in order to perform a fully quantitative determination of tracer binding to its receptor (e.g. TSPO), performing the kinetic modelling of ^{11}C-PK11195 requires a terminal procedure with arterial blood sampling for radioactivity measurement of blood and plasma, since no reference region devoid of TSPO is available within the brain. Due to the longitudinal nature of the study, such methodology was not feasible.

In conclusion, psychosocial stress in rats, in the form of RSD, transiently induces depressive- and anxiety-like behaviour, provokes immune activation in the central nervous system, and significantly diminishes brain glucose metabolism. PET imaging proved a useful tool to noninvasively monitoring the effects of stress in a longitudinal study design. This study supports the hypothesis of a mechanistic role of (neuro)inflammation in the development of depressive behaviour. Nevertheless, further research is warranted to elucidate how the transient effects of psychosocial stress can lead to persistent depressive behaviour, as observed in (treatment-resistant) patients with MDD.

Acknowledgements

The authors would like to thank David Vállez García for the statistical support and Natalia M. Peñaranda Fajardo, for technical assistance in the biochemical analysis.

Disclosure / Conflict of interest

This research did not receive any specific grant from funding agencies in the public, commercial, or not-for-profit sectors. The Authors declare that there is no conflict of interest.

References

1. Marcus M, Yasami T, van Ommeren M, et al. Depression: A Global Public Health Concern Developed. In: *65th World Health Assembly*. Geneva, Switzerland, 2012, pp. 6–8. Palais des Nations, Geneva, Switzerland, 21–26 May 2012.
2. Bschor T, Ising M, Erbe S, et al. Impact of citalopram on the HPA system. A study of the combined DEX/CRH test in 30 unipolar depressed patients. *J Psychiatr Res* 2012; 46: 111–117.
3. Friedman A. Jump-starting natural resilience reverses stress susceptibility. *Science (80)* 2014; 346: 555–555.
4. Cohen S, Janicki-Deverts D, Miller GE. Psychological Stress and Disease. *JAMA* 2007; 298: 1685–1687.
5. de Boer SF, Buwalda B, Koolhaas JM. Untangling the neurobiology of coping styles in rodents: Towards neural mechanisms underlying individual differences in disease susceptibility. *Neurosci Biobehav Rev* 2017; 74: 401–422.
6. Carvalho LA, Juruena MF, Papadopoulos AS, et al. Clomipramine In Vitro Reduces Glucocorticoid Receptor Function in Healthy Subjects but not in Patients with Major Depression. *Neuropsychopharmacology* 2012; 33: 3182–3189.
7. Rossetti AC, Papp M, Gruca P, et al. Stress-induced anhedonia is associated with the activation of the inflammatory system in the rat brain: Restorative effect of pharmacological intervention. *Pharmacol Res* 2016; 103: 1–12.
8. Patki G, Solanki N, Atrooz F, et al. Depression, anxiety-like behavior and memory impairment are associated with increased oxidative stress and inflammation in a rat model of social stress. *Brain Res* 2013; 1539: 73–86.
9. Wohleb ES, McKim DB, Sheridan JF, et al. Monocyte trafficking to the brain with stress and inflammation: a novel axis of immune-to-brain communication that influences mood and behavior. *Front Neurosci* 2015; 8: 1–17.
10. Ramirez K, Niraula A, Sheridan JF. GABAergic modulation with classical benzodiazepines prevent stress-induced neuro-immune dysregulation and behavioral alterations. *Brain Behav Immun* 2015; 51: 1–15.
11. Weber MD, Godbout JP, Sheridan JF. Repeated Social Defeat, Neuroinflammation, and Behavior: Monocytes Carry the Signal. *Neuropsychopharmacology* 2016; 42: 1–51.
12. Loggia ML, Chonde DB, Akeju O, et al. Evidence for brain glial activation in chronic pain patients. *Brain* 2015; 138: 604–615.
13. Czeh M, Gressens P, Kaindl AM. The yin and yang of microglia. *Dev Neurosci* 2011; 33: 199–209.
14. Chijiwa T, Oka T, Lkhagvasuren B, et al. Prior chronic stress induces persistent polyI:C-induced allodynia and depressive-like behavior in rats: Possible involvement of glucocorticoids and microglia. *Physiol Behav* 2015; 147: 264–273.

15. Walker F, Nilsson M, Jones K. Acute and Chronic Stress-Induced Disturbances of Microglial Plasticity, Phenotype and Function. *Curr Drug Targets* 2013; 14: 1262–1276.
16. Venneti S, Lopresti B, Wiley C. Molecular imaging of microglia / macrophages in the brain. *Glia* 2013; 61: 10–23.
17. Beishuizen A, Thijs LG. Endotoxin and the hypothalamo-pituitary-adrenal (HPA) axis. *J Endotoxin Res* 2003; 9: 3–24.
18. Rosenblat JD, Cha DS, Mansur RB, et al. Inflamed moods: A review of the interactions between inflammation and mood disorders. *Prog Neuro-Psychopharmacology Biol Psychiatry* 2014; 53: 23–34.
19. Papadopoulos V, Baraldi M, Guilarte TR, et al. Translocator protein (18kDa): new nomenclature for the peripheral-type benzodiazepine receptor based on its structure and molecular function. *Trends Pharmacol Sci* 2006; 27: 402–409.
20. Parente A, Feltes PK, Vallez Garcia D, et al. Pharmacokinetic Analysis of 11C-PBR28 in the Rat Model of Herpes Encephalitis: Comparison with (R)-11C-PK11195. *J Nucl Med* 2016; 57: 785–791.
21. Vállez García D, Dierckx RAJO, Doorduin J. Three months follow-up of rat mild traumatic brain injury: a combined [18F]FDG and [11C]PK11195 PET study. *J Neurotrauma* 2016; 33: 1–39.
22. Su L, Cai Y, Xu Y, et al. Cerebral metabolism in major depressive disorder: a voxel-based meta-analysis of positron emission tomography studies. *BMC Psychiatry* 2014; 14: 321.
23. McKim DB, Weber MD, Niraula A, et al. Microglial recruitment of IL-1β-producing monocytes to brain endothelium causes stress-induced anxiety. *Mol Psychiatry*; 1–11. Epub ahead of print, 2017. DOI: 10.1038/mp.2017.64.
24. Ramirez K, Fornaguera-Trías J, Sheridan JF. Stress-Induced Microglia Activation and Monocyte Trafficking to the Brain Underlie the Development of Anxiety and Depression. In: *Brain Imaging in Behavioral Neuroscience*, pp. 155–172.
25. Wohleb ES, Hanke ML, Corona AW, et al. β-Adrenergic Receptor Antagonism Prevents Anxiety-Like Behavior and Microglial Reactivity Induced by Repeated Social Defeat. *J Neurosci* 2011; 31: 6277–6288.
26. Wohleb ES, Powell ND, Godbout JP, et al. Stress-Induced Recruitment of Bone Marrow-Derived Monocytes to the Brain Promotes Anxiety-Like Behavior. *J Neurosci* 2013; 33: 13820–13833.
27. Koolhaas JM, Coppens CM, de Boer SF, et al. The Resident-intruder Paradigm: A Standardized Test for Aggression, Violence and Social Stress. *J Vis Exp* 2013; 77 : e4367.
28. Patki G, Solanki N, Atrooz F, et al. Novel mechanistic insights into treadmill exercise based rescue of social defeat-induced anxiety-like behavior and memory impairment in rats. *Physiol Behav* 2014; 130: 135–144.
29. Doorduin J, Klein HC, Dierckx RA, et al. [11C]-DPA-713 and [18F]-DPA-714 as new PET tracers for TSPO: a comparison with [11C]-(R)-PK11195 in a rat model of herpes encephalitis. *Mol Imaging Biol* 2009; 11: 386–398.
30. Serra M, Pisu MG, Floris I, et al. Social isolation-induced changes in the hypothalamic–pituitary–adrenal axis in the rat. *Stress* 2005; 8: 259–264.
31. Buwalda B, Geerdink M, Vidal J, et al. Social behavior and social stress in adolescence: A focus on animal models. *Neurosci Biobehav Rev* 2011; 35: 1713–1721.
32. Ma X, Jiang D, Jiang W, et al. Social Isolation-Induced Aggression Potentiates Anxiety and Depressive-Like Behavior in Male Mice Subjected to Unpredictable Chronic Mild Stress. *PLoS One* 2011; 6: e20955.
33. Kilkenny C, Browne WJ, Cuthill IC, et al. Improving Bioscience Research Reporting: The ARRIVE Guidelines for Reporting Animal Research. *PLoS Biol* 2010; 8: e1000412.
34. Hurley LL, Akinfiresoye L, Kalejaiye O, et al. Antidepressant effects of resveratrol in an animal model of depression. *Behav Brain Res* 2014; 268: 1–7.
35. Walf AA, Frye CA. The use of the elevated plus maze as an assay of anxiety-related behavior in rodents. *Nat Protoc* 2007; 2: 322–328.
36. Gonzalez LE, File SE. A five minute experience in the elevated plus-maze alters the state of the benzodiazepine receptor in the dorsal raphe nucleus. *J Neurosci* 1997; 17: 1505–1511.

37. Dere E, Huston JP, De Souza Silva MA. The pharmacology, neuroanatomy and neurogenetics of one-trial object recognition in rodents. *Neurosci Biobehav Rev* 2007; 31: 673–704.
38. Elizalde N, Gil-Bea FJ, Ramírez MJ, et al. Long-lasting behavioral effects and recognition memory deficit induced by chronic mild stress in mice: effect of antidepressant treatment. *Psychopharmacology (Berl)* 2008; 199: 1–14.
39. Hovens IB, van Leeuwen BL, Nyakas C, et al. Prior infection exacerbates postoperative cognitive dysfunction in aged rats. *Am J Physiol - Regul Integr Comp Physiol* 2015; 309: R148–R159.
40. Antunes M, Biala G. The novel object recognition memory: neurobiology, test procedure, and its modifications. *Cogn Process* 2012; 13: 93–110.
41. Wong K-P, Sha W, Zhang X, et al. Effects of Administration Route, Dietary Condition, and Blood Glucose Level on Kinetics and Uptake of 18F-FDG in Mice. *J Nucl Med* 2011; 52: 800–807.
42. Vállez García D, Casteels C, Schwarz AJ, et al. A Standardized Method for the Construction of Tracer Specific PET and SPECT Rat Brain Templates : Validation and Implementation of a Toolbox. *PLoS One* 2015; 10: 1–21.
43. Schwarz AJ, Danckaert A, Reese T, et al. A stereotaxic MRI template set for the rat brain with tissue class distribution maps and co-registered anatomical atlas: Application to pharmacological MRI. *Neuroimage* 2006; 32: 538–550.
44. Boellaard R, Delgado-Bolton R, Oyen WJ, et al. FDG PET/CT: EANM procedure guidelines for tumour imaging: version 2.0. *Eur J Nucl Med Mol Imaging* 2015; 42: 328–354.
45. Setiawan E, Wilson AA, Mizrahi R, et al. Role of Translocator Protein Density, a Marker of Neuroinflammation, in the Brain During Major Depressive Episodes. *JAMA Psychiatry* 2015; 72: 268.
46. Weber MD, Godbout JP, Sheridan JF. Repeated Social Defeat, Neuroinflammation, and Behavior: Monocytes Carry the Signal. *Neuropsychopharmacology* 2017; 42: 46–61.
47. Kim Y-K, Won E. The influence of stress on neuroinflammation and alterations in brain structure and function in major depressive disorder. *Behav Brain Res* 2017; 329: 6–11.
48. Phillips JR, Hewedi DH, Eissa AM, et al. The cerebellum and psychiatric disorders. *Front public Heal* 2015; 3: 66.
49. Wei K, Xue H, Guan Y, et al. Analysis of glucose metabolism of 18F-FDG in major depression patients using PET imaging: Correlation of salivary cortisol and α-amylase. *Neurosci Lett* 2016; 629: 52–57.
50. Hinwood M, Tynan RJ, Day TA, et al. Repeated Social Defeat Selectively Increases FosB Expression and Histone H3 Acetylation in the Infralimbic Medial Prefrontal Cortex. *Cereb Cortex* 2011; 21: 262–271.
51. Yu T, Guo M, Garza J, et al. Cognitive and neural correlates of depression-like behaviour in socially defeated mice: an animal model of depression with cognitive dysfunction. *Int J Neuropsychopharmacol* 2011; 14: 303–317.
52. Marx C, Lex B, Calaminus C, et al. Conflict Processing in the Rat Brain: Behavioral Analysis and Functional μPET Imaging Using [F]Fluorodeoxyglucose. *Front Behav Neurosci* 2012; 6: 4.
53. Lehnert W, Gregoire M-C, Reilhac A, et al. Characterisation of partial volume effect and region-based correction in small animal positron emission tomography (PET) of the rat brain. *Neuroimage* 2012; 60: 2144–2157.
54. Ledeboer A, Sloane EM, Milligan ED, et al. Minocycline attenuates mechanical allodynia and proinflammatory cytokine expression in rat models of pain facilitation. *Pain* 2005; 115: 71–83.
55. Studebaker GA. A 'Rationalized' Arcsine Transform. *J Speech Lang Hear Res* 1985; 28: 455–462.
56. Mikaelsson MA, Constância M, Dent CL, et al. Placental programming of anxiety in adulthood revealed by Igf2-null models. *Nat Commun* 2013; 4: 2311.
57. Francis G. Equivalent statistics and data interpretation. *Behav Res Methods*. Epub ahead of print, 2016. DOI: 10.3758/s13428-016-0812-3.
58. Johnson KE, McMorris BJ, Raynor LA, et al. What big size you have! Using effect sizes to

determine the impact of public health nursing interventions. *Appl Clin Inform* 2013; 4: 434–444.
59. Hardin JW, Hilbe JM. *Generalized Estimating Equations*. 2nd ed. Boca Raton, FL: Chapman & Hall/CRC, 2012.
60. Streiner DL. Best (but oft-forgotten) practices: The multiple problems of multiplicity-whether and how to correct for many statistical tests. *Am J Clin Nutr* 2015; 102: 721–728.
61. Pulliam J, Dawaghreh A, Alema-Mensah E, et al. Social Defeat Stress Produces Prolonged Alterations in Acoustic Startle and Body Weight Gain in Male Long Evans Rats. *J Psychiatr Res* 2010; 44: 1–14.
62. Koolhaas JM, Meerlo P, De Boer SF, et al. The temporal dynamics of the stress response. *Neurosci Biobehav Rev* 1997; 21: 775–782.
63. Harris R. Chronic and acute effects of stress on energy balance: are there appropriate animal models? *Am J Physiol Comp Physiol* 2015; 308: R250–R265.
64. Atsak P, Hauer D, Campolongo P, et al. Glucocorticoids interact with the hippocampal endocannabinoid system in impairing retrieval of contextual fear memory. *Proc Natl Acad Sci* 2012; 109: 3504–3509.
65. Vargas-López V, Torres-Berrio A, González-Martínez L, et al. Acute restraint stress and corticosterone transiently disrupts novelty preference in an object recognition task. *Behav Brain Res* 2015; 291: 60–66.
66. Luine V. Recognition memory tasks in neuroendocrine research. *Behav Brain Res* 2015; 285: 158–164.
67. McKim DB, Niraula A, Tarr AJ, et al. Neuroinflammatory Dynamics Underlie Memory Impairments after Repeated Social Defeat. *J Neurosci* 2016; 36: 2590–2604.
68. McEwen B, Morrison J. The Brain on Stress: Vulnerability and Plasticity of the Prefrontal Cortex over the Life Course. *Neuron* 2013; 79: 16–29.
69. Cheng W, Rolls ET, Qiu J, et al. Medial reward and lateral non-reward orbitofrontal cortex circuits change in opposite directions in depression. *Brain* 2016; 139: 3296–3309.
70. Belin-Rauscent A, Daniel M-L, Puaud M, et al. From impulses to maladaptive actions: the insula is a neurobiological gate for the development of compulsive behavior. *Mol Psychiatry* 2015; 21: 1–9.
71. Strange BA, Witter MP, Lein ES, et al. Functional organization of the hippocampal longitudinal axis. *Nat Rev Neurosci* 2014; 15: 655–669.
72. Eichenbaum H, Yonelinas AR, Ranganath C. The Medial Temporal Lobe and Recognition Memory. *Annu Rev Neurosci* 2007; 30: 123–152.
73. Shelton RC, Claiborne J, Sidoryk-Wegrzynowicz M, et al. Altered expression of genes involved in inflammation and apoptosis in frontal cortex in major depression. *Mol Psychiatry* 2011; 16: 751–762.
74. Frank MG, Watkins LR, Maier SF. Stress- and glucocorticoid-induced priming of neuroinflammatory responses: Potential mechanisms of stress-induced vulnerability to drugs of abuse. *Brain Behav Immun* 2011; 25: S21–S28.
75. Frank MG, Baratta M V., Sprunger DB, et al. Microglia serve as a neuroimmune substrate for stress-induced potentiation of CNS pro-inflammatory cytokine responses. *Brain Behav Immun* 2007; 21: 47–59.
76. Sorrells SF, Caso JR, Munhoz CD, et al. The Stressed CNS: When Glucocorticoids Aggravate Inflammation. *Neuron* 2009; 64: 33–39.
77. Wohleb ES, McKim DB, Shea DT, et al. Re-establishment of Anxiety in Stress-Sensitized Mice Is Caused by Monocyte Trafficking from the Spleen to the Brain. *Biol Psychiatry* 2014; 75: 970–981.
78. Wohleb ES, Fenn AM, Pacenta AM, et al. Peripheral innate immune challenge exaggerated microglia activation, increased the number of inflammatory CNS macrophages, and prolonged social withdrawal in socially defeated mice. *Psychoneuroendocrinology* 2012; 37: 1491–1505.
79. Devinsky O, Morrell MJ, Vogt BA. Contributions of anterior cingulate cortex to behaviour. *Brain* 1995; 118: 279–306.
80. Saxena S, Brody AL, Ho ML, et al. Cerebral metabolism in major depression and obsessive-

compulsive disorder occurring separately and concurrently. *Biol Psychiatry* 2001; 50: 159–170.
81. Martinot J, Hardy P, Feline A. Left prefrontal glucose hypometabolism in the depressed state: a confirmation. *Am J Psychiatry* 1990; 147: 1313–1317.
82. Biver F, Goldman S, Delvenne V, et al. Frontal and Parietal Metabolic Disturbances in Unipolar Depression. *Biol Psychiatry* 1994; 36: 381–388.
83. Liu B, Le KX, Park M, et al. In Vivo Detection of Age- and Disease-Related Increases in Neuroinflammation by 18 F-GE180 TSPO MicroPET Imaging in Wild-Type and Alzheimer's Transgenic Mice. *J Neurosci* 2015; 35: 15716–15730.
84. Schuitemaker A, van der Doef TF, Boellaard R, et al. Microglial activation in healthy aging. *Neurobiol Aging* 2012; 33: 1067–1072.
85. Choi H, Choi Y, Kim KW, et al. Maturation of metabolic connectivity of the adolescent rat brain. *Elife* 2015; 4: 1–12.
86. Buwalda B, Stubbendorff C, Zickert N, et al. Adolescent social stress does not necessarily lead to a compromised adaptive capacity during adulthood: A study on the consequences of social stress in rats. *Neuroscience* 2013; 249: 258–270.
87. Vállez Garcia D, F J De Vries E, Toyohara J, et al. Evaluation of [11C]CB184 for imaging and quantification of TSPO overexpression in a rat model of herpes encephalitis. *Eur J Nucl Med Mol Imaging* 2015; 42: 1106–1118.
88. Boutin H, Prenant C, Maroy R, et al. [18F]DPA-714: Direct Comparison with [11C]PK11195 in a Model of Cerebral Ischemia in Rats. *PLoS One 2013*; 8: e56441.
89. Lodge MA. Repeatability of SUV in Oncologic 18 F-FDG PET. *J Nucl Med* 2017; 58: 523–532.
90. Adams MC, Turkington TG, Wilson JM, et al. A Systematic Review of the Factors Affecting Accuracy of SUV Measurements. *Am J Roentgenol* 2010; 195: 310–320.

Supplementary material

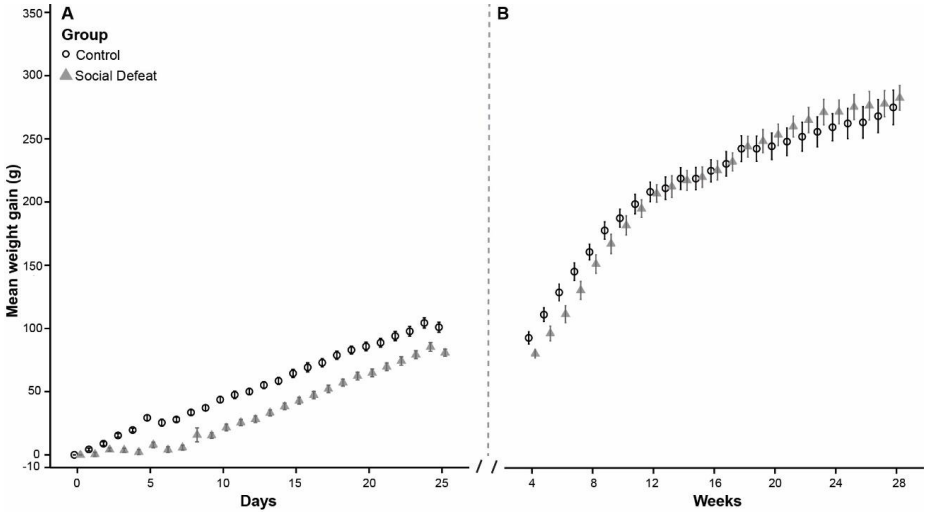

Supplementary figure 1: (A) Bodyweight gain (g) of control (n=18) and SoD rats (n=19) from day 0 to 25 of the short-term protocol, with significant decreased bodyweight gain in SoD rats evident already on day 2 (p<0.01) and with no recovery up to day 25 (p<0.001); **(B)** No significant difference in bodyweight gain (g) of control (n=8) and SoD rats (n=9) was found from week 5 to 28 of the follow-up protocol.

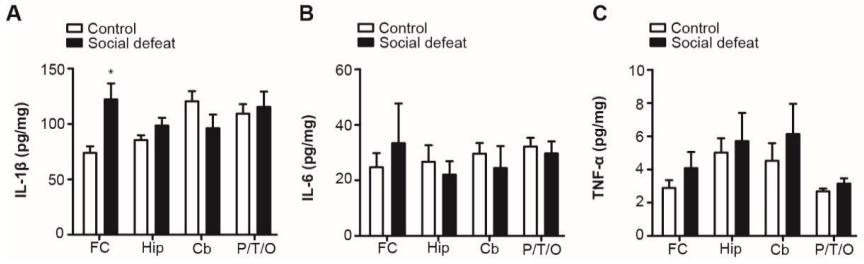

Supplementary figure 2: Assessment of the pro-inflammatory cytokines in the frontal cortex (FC), hippocampus (Hip), cerebellum (Cb) and parietal/temporal/occipital cortex (P/T/O) in the brains of control and defeated rats on day 25. **(A)** IL-1β levels were increased in the frontal cortex of SoD rats, *p<0.05. No significant differences were found in the other investigated brain areas. **(B)** Quantification of IL-6 revealed no significant differences between groups in any brain regions. A moderate effect size was found in the frontal cortex (d=0.63) of SoD rats. **(C)** TNF-α levels did not differ between groups in any brain regions; a moderate effect size was found in the frontal cortex of SoD rats (d=0.55).